

Return Encls

CALIFORNIA INSTITUTE OF TECHNOLOGY

ANTENNA LABORATORY

Technical Report No. 92

ELECTROMAGNETIC WAVE PROPAGATION
IN ALMOST PERIODIC MEDIA

by

A. R. Mickelson and D. L. Jaggard

copy

MS

ELECTROMAGNETIC WAVE PROPAGATION
IN ALMOST PERIODIC MEDIA

A. R. Mickel'son and D. L. Jaggard

Antenna Laboratory

Report No. 92

California Institute of Technology

ABSTRACT

The problem of electromagnetic wave propagation in almost periodic media is investigated and a solution is obtained directly from Maxwell's equations. The evaluation of this solution involves a generalization to almost periodic media of the Brillouin diagram of periodic media. The Brillouin diagram is used to place in evidence similarities and differences of wave propagation in periodic and almost periodic media. It is shown that although the periodic and almost periodic theories agree in many cases of interest there exist cases in which distinct differences appear.

Electromagnetic Wave Propagation in Almost Periodic Media

I. INTRODUCTION

In this paper it is our purpose to integrate the abstract theory of almost periodic functions with electromagnetic wave propagation theory. We present a theory of wave propagation in almost periodic media and compare the electromagnetic properties of these media with those of the better understood periodic media. This study is motivated by a desire to find a deterministic model medium which takes into account the practical limitations on the perfect phase coherence of periodic models. As will be shown, the electromagnetic response of almost periodic structures is invariant under phasing of the amplitudes of the structure's constituent frequency components, and therefore these structures are natural candidates for the desired models.

It was in 1923 that Harold Bohr found the almost periodic generalization of Fourier series [1,2]. Subsequent work by Bohr [3-5] led Besicovitch [6], Bochner [7] and Favard [8] to various simplifications of the theory soon after its inception. In 1926 and 1927 Favard extended the theory by considering the case of linear differential equations with almost periodic coefficients [9,10]. Following the initial work in the 1920's and 1930's, interest in the theory of almost periodic functions was dormant until problems in stability theory renewed work in this subject during the 1960's [11]. Books by Bohr [12], Besicovitch [13] and Wiener [14] provide readily available introductions to the subject. An extensive bibliography is given in the lecture notes by Fink [15].

According to Bohr, an almost periodic function is one which can be resolved into "pure vibrations" [12]. This implies that the spectrum of an almost periodic function is composed of discrete lines, or equivalently, that an almost periodic function $f(z)$ can be defined by the relation

$$f(z) = \sum_M a_M \exp(i\kappa_M z) \quad (1)$$

where the κ_M 's are real and the harmonic strengths a_M are complex. For the case when all κ_M 's are commensurable, $f(z)$ becomes a periodic function.

The functions plotted in Figure 1 a,b exhibit the characteristics of periodic and almost periodic functions, respectively. Each function $f(z)$ is composed of three "pure vibrations" or "tones," namely

$$f(z) = f_P(z) = \cos[\pi z] + \cos[3\pi z] + \cos[5\pi z] \quad (2)$$

in Figure 1 a and

$$f(z) = f_{AP}(z) = \cos[\pi z] + \cos[3(1.7)\pi z/3^{3/2}] \\ + \cos[(5)3^{3/2}\pi z/1.7] \quad (3)$$

in Figure 1 b. The functions are of similar form. However, the difference between the periodic and almost periodic case is immediately apparent from the plots.

Almost periodic functions arise in a variety of situations. For example, amplitude and frequency modulated signals are represented as almost periodic functions. Many man-made structures that are presumed periodic are actually almost periodic due to phase or amplitude variations. Naturally occurring almost periodic structures such as disordered crystal lattices can be described by the theory presented here or its extension.

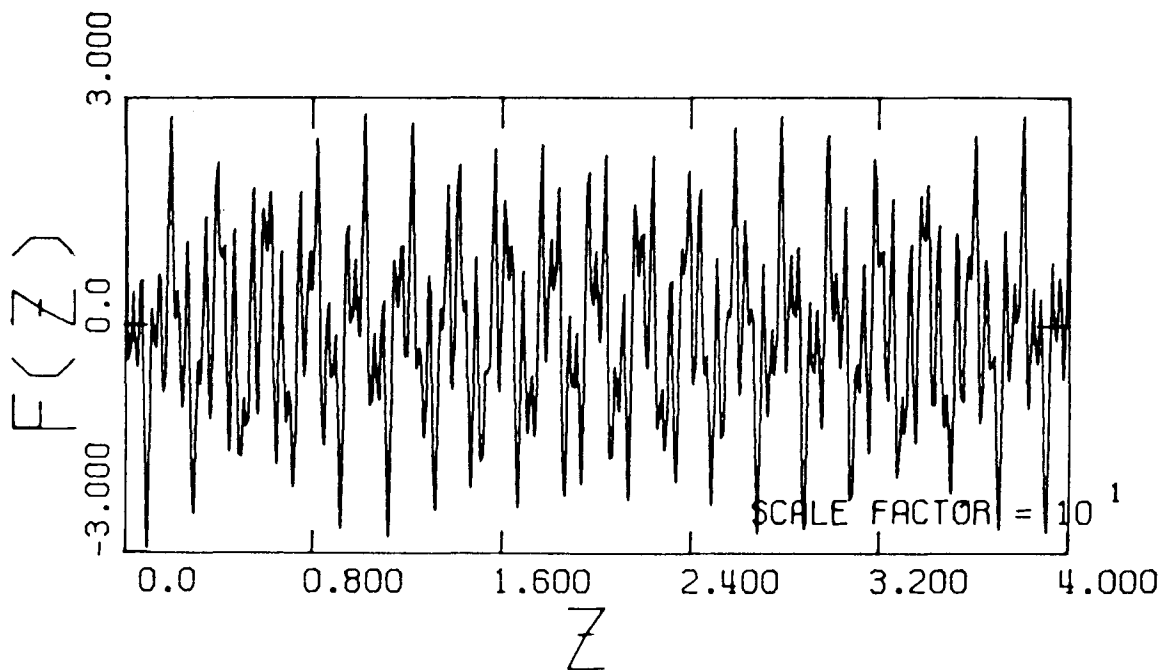
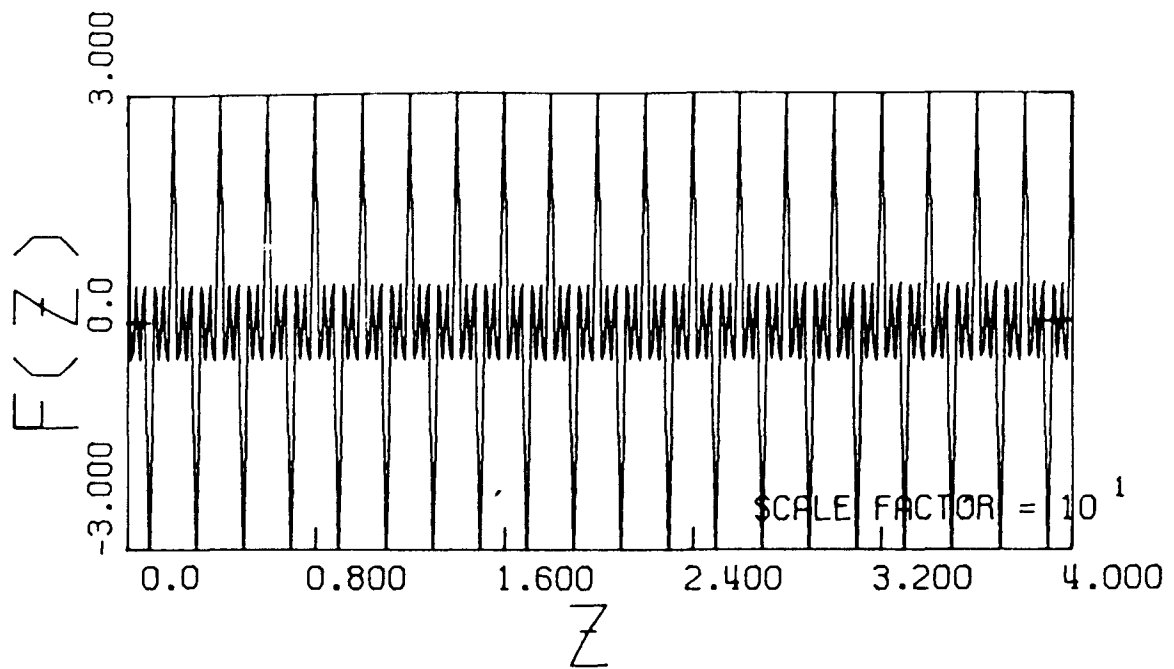


Figure 1. A comparison of a periodic function (a) $f(z) = f_p(z)$ with an almost periodic function (b) $f(z) = f_{AP}(z)$ where $f_p(z) = \cos[\pi z] + \cos[3\pi z] + \cos[5\pi z]$ and $f_{AP}(z) = \cos[\pi z] + \cos[3(1.7)\pi z/3^{1/2}] + \cos[(5)3^{1/2}\pi z/1.7]$.

In section II we set up the problem under consideration. A method of solution is proposed and carried out. Brillouin or dispersion diagrams are employed to implement the solution in section III. The last section contains comments concerning the distinctions between electromagnetic wave propagation in periodic and almost periodic media.

II. PROBLEM STATEMENT AND SOLUTION

As an archetypical problem, consider the propagation of electromagnetic waves in a longitudinally almost periodic medium as shown in Figure 2. The transverse components ψ of the electric field satisfy the Helmholtz equation which, in this case, becomes the almost periodic Mathieu equation

$$\left[\frac{d^2}{dz^2} + k^2 \epsilon(z) \right] \psi(z) = 0 \quad (4)$$

where the free space wavenumber is k and the dielectric permittivity $\epsilon(z)$ is given by the periodic or almost periodic function

$$\epsilon(z) = \epsilon_r \left[\sum_{M=1}^P \eta_M e^{i\kappa_M z} + \sum_{M=-P}^{-1} \eta_M e^{i\kappa_M z} \right] \quad (5)$$

For real dielectric permittivity $\eta_M = \eta_{-M}^*$, where the asterisk denotes complex conjugation. For periodic media, the spatial frequencies κ_M satisfy the relation $\kappa_M = M\kappa$ ($M = \text{integer}$) whereas for almost periodic media the ratio κ_i/κ_j is an irrational number for at least one pair of indices i, j ($i \neq j$). For simplification, one assumes that the relative dielectric constant ϵ_r and the perturbation parameters η_M are real. The generalization to complex numbers is straightforward and can be carried out as in the periodic case [18,19].

Applying the Fourier transform to equations (4) and (5) one obtains

$$\gamma^2 \psi(\gamma) - \frac{k^2 \epsilon_r}{2} \sum_M \eta_M \hat{\psi}(\gamma + \kappa_M) = 0 \quad (6)$$

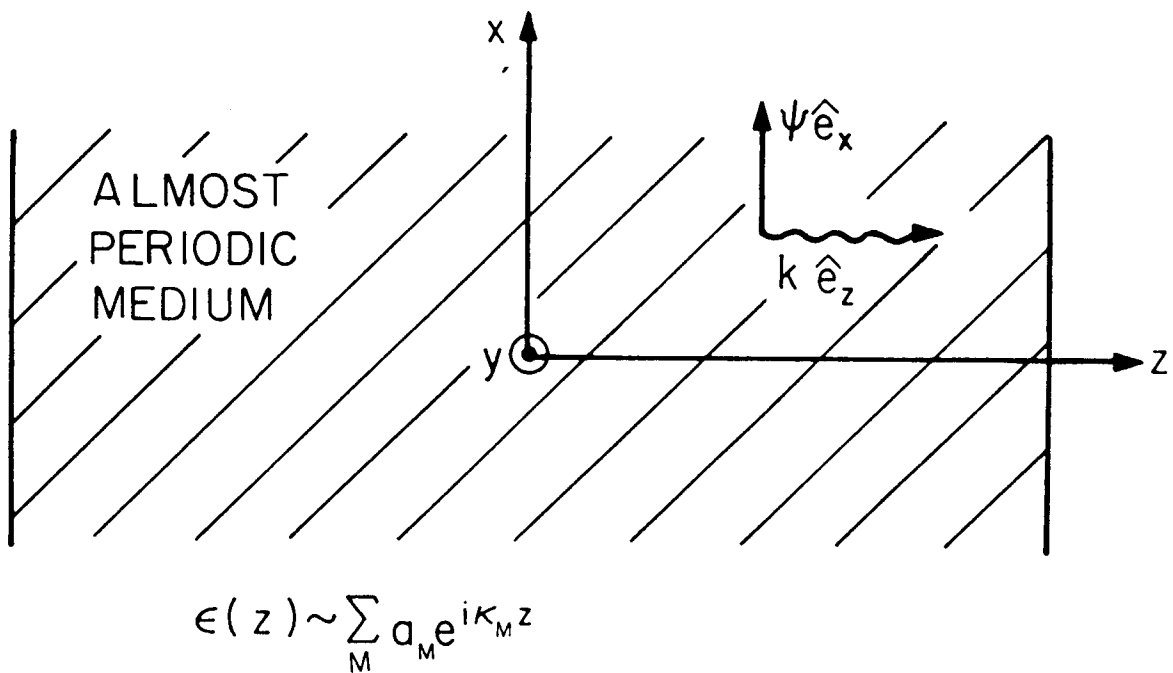


Figure 2. Geometry of plane wave in almost periodic dielectric medium. The transverse component of the electric field (say in the \hat{e}_x direction) is given by $\psi \hat{e}_x$. The wave vector \underline{k} is along the \hat{e}_z direction. The permittivity $\epsilon(z)$ is proportional to a sum of exponentials of various spatial frequencies κ_M .

where γ is the transform variable and the circumflex denotes the Fourier transform. This process transforms the original second order differential equation (4) into a non-local algebraic equation (6). The non-local algebraic equation can be reduced to an infinite set of local algebraic equations by assuming a solution to (6) of the form

$$\psi(\gamma) = \sum_{M_1=-\infty}^{\infty} \sum_{M_2=-\infty}^{\infty} \dots \sum_{M_p=-\infty}^{\infty} a_{M_1, M_2, \dots, M_p} \hat{f}(\gamma + M_1 \kappa_1 + M_2 \kappa_2 + \dots + M_p \kappa_p) \quad (7)$$

For concreteness, assume that the dielectric permittivity is composed of two "pure vibrations" or "tones", namely

$$\left. \begin{aligned} p &= 2 \\ \eta_1 &= \eta_{-1} \\ \eta_2 &= \eta_{-2} \\ \eta_0 &= 1 \end{aligned} \right\} \quad (8)$$

Substituting (8) in ansatz (7), one sees the solution to (6) can be written as

$$\hat{\psi}(\gamma) = \begin{cases} \sum_M a_M \hat{f}(\gamma + M \kappa) & \text{periodic} \\ \sum_{M, N} a_{MN} \hat{f}(\gamma + M \kappa_1 + N \kappa_2) & \text{almost periodic} \end{cases} \quad (9)$$

In configuration space this solution becomes

$$\psi(z) = \begin{cases} \sum_M a_M \exp[i(M \kappa \cdot z)] f(z) & \text{periodic} \\ \sum_{M, N} a_{MN} \exp[i(M \kappa_1 \cdot z + N \kappa_2 \cdot z)] f(z) & \text{almost periodic} \end{cases} \quad (10)$$

Note that equation (8a) represents the Floquet solution for periodic media as expected. We assert that (8b) gives the necessary generalization for the almost periodic case. The proposed solution (10) agrees in form with that found by Abel [16,17] who employed a different method in his derivation.

The function $f(z)$ given in (10) is now taken to be

$$f(z) = \exp(i\beta z), \quad (11)$$

β being the wavenumber in the medium. By combining (10) and (11) and substituting into (4), one finds that for an almost periodic medium (i.e. κ_1 and κ_2 incommensurable)

$$\begin{aligned} [k^2 \epsilon_r - (\beta + M\kappa_1 + N\kappa_2)^2] a_{MN} + k^2 \epsilon_r [\eta_1 (a_{M-1,N} + a_{M+1,N}) \\ + \eta_2 (a_{M,N-1} + a_{M,N+1})] = 0 \\ M, N = (\dots, -2, -1, 0, 1, 2, \dots) \end{aligned} \quad (12)$$

This is the infinite set of local algebraic equations mentioned previously (7). Since the space harmonics a_{MN} form a countable set, they can always be mapped into a one-dimensional vector to obtain (12) in the familiar form

$$\underline{D} \cdot \underline{a} = 0 \quad (13)$$

where \underline{D} is a matrix and \underline{a} a column vector of the space harmonics. Clearly, the wavenumber β must satisfy the dispersion relation

$$\det \underline{D} = 0 \quad (14)$$

By backsubstituting β into \underline{D} the \underline{a} 's can be obtained as a one-parameter family.

The entire process is analogous to the periodic case where $\underline{D} = \underline{D}_p$ and $\underline{a} = \underline{a}_p$ given by [21]

$$\underline{D}_p = \begin{bmatrix} f_1 & D_{-2} & f_1 & f_2 & & & & \\ f_2 & f_1 & D & f_1 & f_2 & & & \\ & f_2 & f_1 & D_0 & f_1 & f_2 & & \\ & & & f_2 & f_1 & D_1 & f_1 & f_2 \\ \bullet & \bullet & & & f_2 & f_1 & D_2 & f_1 \\ & & & & & & & & \bullet \\ & & & & & & & & & \bullet \end{bmatrix} \quad (15)$$

where $D_N = 1 - (\beta + N\kappa)^2 / k^2 \epsilon_r$

$$f_N = \eta_N / 2$$

$$\text{and } \underline{a}_p = [\dots a_{-2}, a_{-1}, a_0, a_1, a_2 \dots]^T \quad (16)$$

where T denotes the matrix transpose.

We now define a plane to line mapping which will enable us to define the matrix \underline{D}_{AP} and the corresponding column vector \underline{a}_{AP} . The basic scheme is illustrated in Figure 3. A grid is drawn with the grid points labeled by their integer coordinates (i, j) . The boxes are formed by lines passing through points equidistant from the origin $(0, 0)$ in the sense that the distance from point 1 to point 2 is defined by

$$d_{12} = |i_1 - i_2| + |j_1 - j_2| \quad (17)$$

The boxes are labeled according to the order in which they would be traversed outward from the origin, analogously to the labeling of Brillouin zones in a plane [23] as shown in Figure 3a. The points on or within the i^{th} box

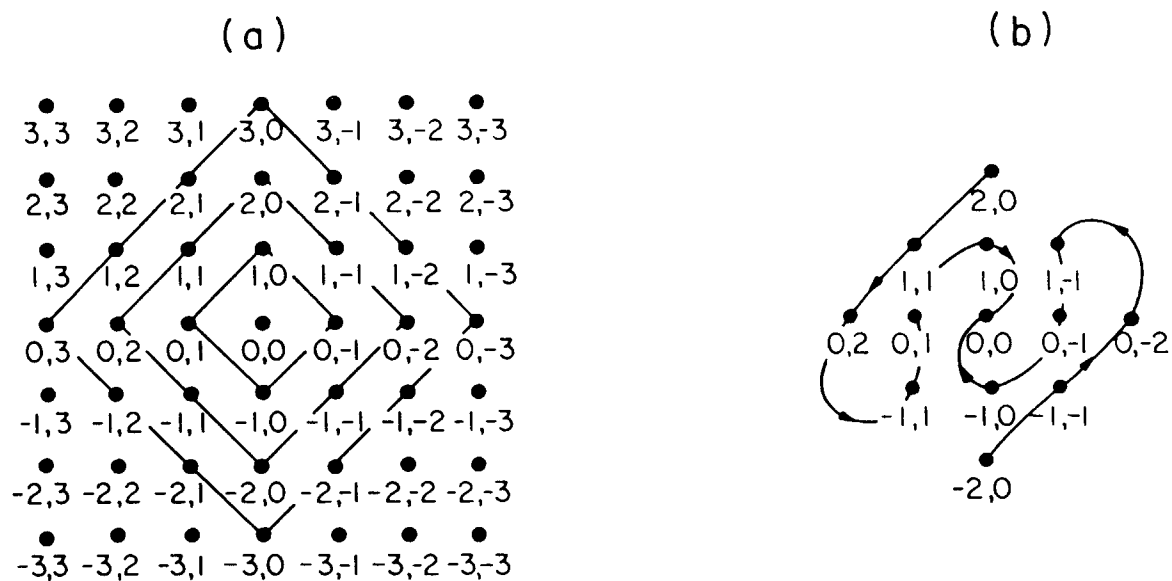


Figure 3. Scheme for plane to line mapping. (a) The grid points (i,j) are connected by boxes which denote the order of the theory starting with the smallest Δ_{ij} around the origin. (b) The ordering of the grid points necessary to complete the mapping.

are denoted i^{th} order points and will be used to construct an i^{th} order theory. The points to the right of the origin are defined to include those points directly below the origin and the points to the left of the origin to include those points that lie directly above the origin. To specify a given order mapping, it remains only to specify the order in which the points to the right and the points to the left must be taken. This is illustrated in Figure 3b for the second order mapping. The general rule for points to the right (for a given order $2N$) is to begin directly below the origin on the surface of the $2N^{\text{th}}$ box, follow the box around to the last point on the right, drop directly below to the $(2N-1)^{\text{th}}$ box, follow it around to the last point on the right and jump above to the $(2N-2)^{\text{th}}$ box, continuing the procedure to the origin. Odd order mappings and points to the left are mapped analogously.

Employing this mapping we find

$$\underline{a}_{AP}^{(1)} = \begin{bmatrix} D_{01} & & & & & & f_2 \\ & D_{10} & & & & & f_1 \\ f_2 & f_1 & D_{00} & f_1 & f_2 & & \\ & & f_1 & D_{-10} & & & \\ & & f_2 & & & & D_{0-1} \end{bmatrix} \quad (18)$$

where $D_{NM} = 1 - (\beta + M\kappa_1 + N\kappa_2)^2 / k^2 \epsilon_r$

$$f_N = \eta_N / 2$$

and $\underline{a}_{AP}^{(1)} = [a_{01}, a_{10}, a_{00}, a_{-10}, a_{0-1}]^T \quad (19)$

for the first order mapping indicated by the superscript. Our investigations will be centered exclusively on this first order theory. The second order quantities are given elsewhere [20]. We note that for the first order theory, $\underline{D}_{AP}^{(1)}$ is a 5 x 5 matrix whereas for the second order theory $\underline{D}_{AP}^{(2)}$ has ballooned to a 13 x 13 matrix. In general, the order of \underline{D}_{AP} , denoted by $O(\underline{D}_{AP})$, is given for the N^{th} order theory by

$$O(\underline{D}_{AP}) = 1 + 2 N(N+1) \quad (21)$$

One can observe the relative sparseness of the almost periodic matrix \underline{D}_{AP} with respect to its periodic counter part. For example, using two tones and first order theory we find in the periodic case.

$$\underline{D}_P^{(1)} = \begin{bmatrix} D_2 & f_1 & f_2 & & \\ f_1 & D_1 & f_1 & & \\ f_2 & f_1 & D_0 & f_1 & f_2 \\ & f_2 & f_1 & D_{-1} & f_1 \\ & & f_2 & f_1 & D_{-2} \end{bmatrix} \quad (22)$$

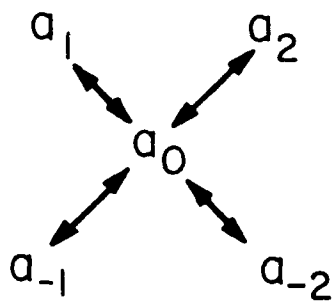
and

$$\underline{a}_P^{(1)} = [a_2, a_1, a_0, a_{-1}, a_{-2}]^T \quad (23)$$

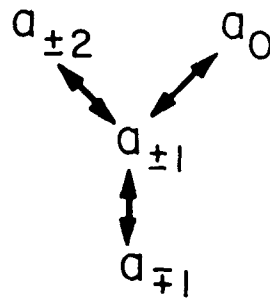
It is immediately apparent that the periodic matrix \underline{D}_P is a fuller matrix than \underline{D}_{AP} . The physical content of this fact can be found by considering the coupling scheme of periodic and almost periodic cases.

By comparing matrix (19) with (22) one notes that in the first order theory, coupling between space harmonics can only occur through the D_{00}

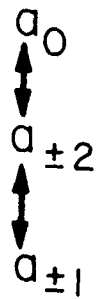
element of the matrix or the a_{00} component of the column vector for almost periodic media whereas in the periodic case the coupling can occur in a variety of ways. This difference in coupling schemes is most easily seen by comparing Figure 4 with Figure 5. The first of these figures represents coupling in the periodic case which has been described by equations (22) and (23). The double arrowed line shows the allowable direct couplings between various space harmonics. The second of these figures represents coupling in the almost periodic case which has been described by equations (19) and (20). We conclude from a comparison of Figures 4 and 5 or matrices (22) and (17) that the periodic medium leads to a richer coupling scheme in the first order theory. The same observation holds for higher order theories. In the almost periodic case, the various perturbations act almost independently in contradistinction to the periodic case. This latter point will be examined further in the next section.



(a)



(b)



(c)

Figure 4. Coupling scheme of the first order space harmonics for the case of a periodic medium composed of two tones.

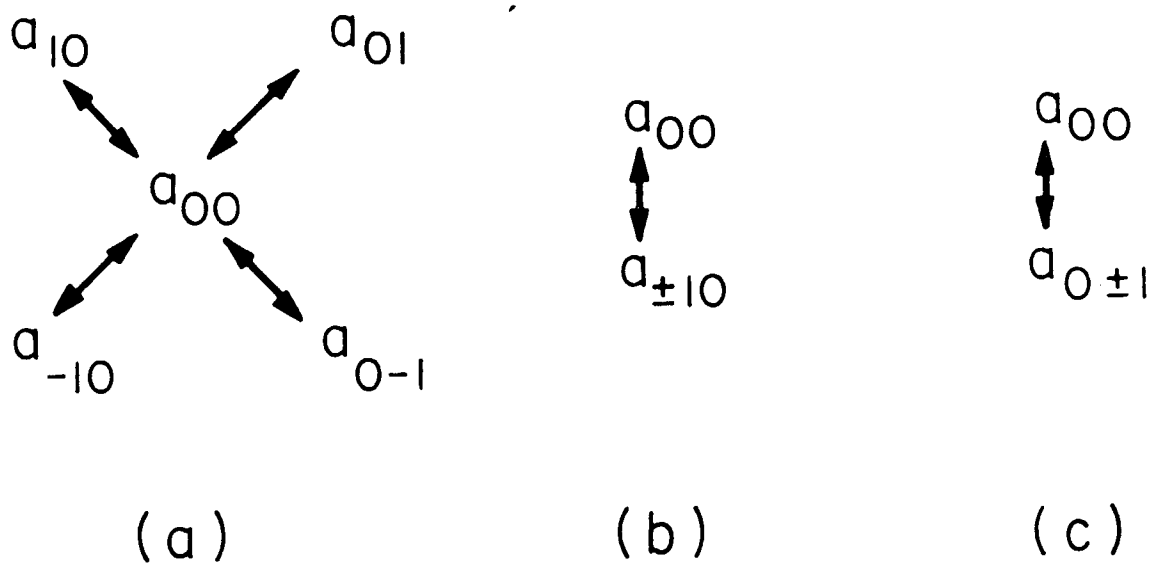


Figure 5. Coupling scheme of the first order space harmonics for the case of an almost periodic medium composed of two tones.

III. BRILLOUIN DIAGRAMS

In this section we will use Brillouin diagrams to manifest the properties of almost periodic media. In particular, the frequencies and relative coupling strengths of interactions between different space harmonics will be demonstrated. The utility of this approach is that the Brillouin diagram produces a rule-of-thumb pictorial device which not only indicates important coupling effects but also gives us an expectation for results of physical measurements such as the reflection coefficient. It is in this physically motivated spirit that we proceed.

Using the ordering presented in the previous section, we find the Brillouin diagram for an almost periodic medium composed of two tones κ_1 and κ_2 as the perturbations η_1 and η_2 approach zero. The result is given in Figure 6 which includes all space harmonics necessary for the first and second order theories.

From the dispersion relation (14) and the matrix (18) the polynomial in β^2 representing the dispersion relation is given by

$$\begin{aligned} D_{0-1} D_{-10} D_{00} D_{10} D_{01} - |f_1|^2 D_{01} D_{0-1} (D_{10} + D_{10}) \\ - |f_2|^2 D_{10} D_{-10} (D_{01} + D_{0-1}) = 0 \end{aligned} \quad (23)$$

for the first order theory.

A comparison of periodic and almost period media with two widely spaced tones is plotted in the Brillouin diagrams of Figures 7 and 8.

The test medium for these figures has a dielectric permittivity

$$\epsilon(z) \approx \epsilon_r [1 + \eta_1 \cos \kappa_1 z + \eta_2 \cos \kappa_2 z] \quad (24)$$

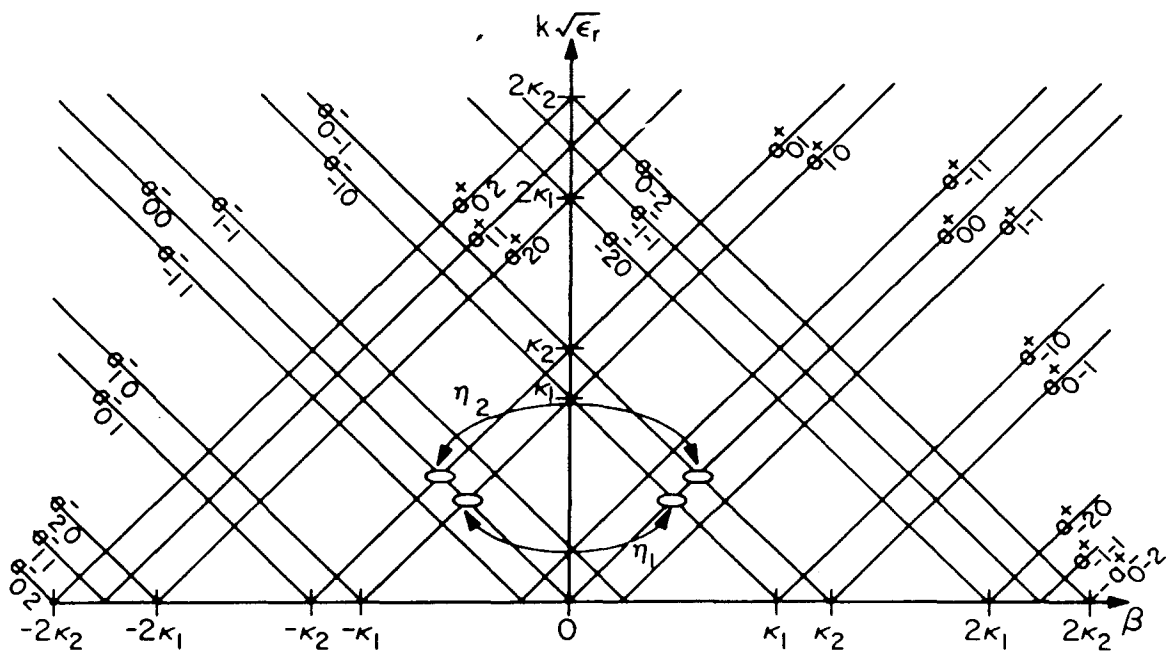


Figure 6. Second order Brillouin (dispersion) diagram for an almost periodic medium composed of two closely spaced tones as the perturbation approaches zero. The tones are characterized by the spatial frequencies κ_1 and κ_2 and perturbation strengths η_1 and η_2 . The free space wave number (i.e., normalized frequency) is given by k , the wave number in the medium by β and the average relative dielectric constant by ϵ_r . The arrows show the direct couplings between sets of space harmonics which can occur.

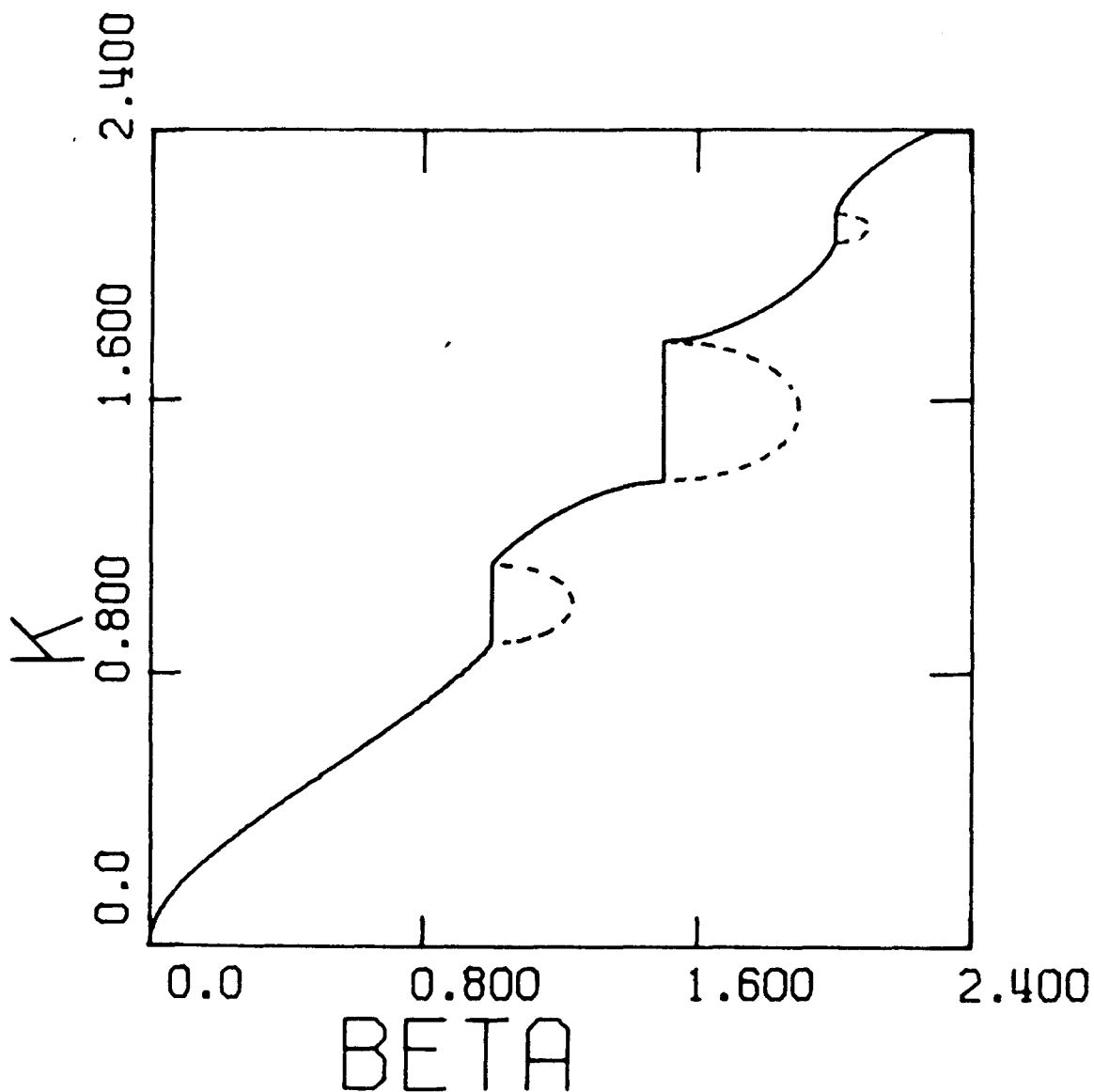


Figure 7. A plot of the Brillouin diagram for the periodic medium described by $\epsilon(z) = \epsilon_r [1 + 0.5 \cos(\kappa_1 z) + 0.5 \cos(\kappa_2 z)]$ where $\kappa_1 = 1.0$ and $\kappa_2 = 1.5$. The solid line represents values of $\text{Re}\{\beta\}$. The symbol K is defined by $K = k\epsilon_r^{3/2}$ on this graph. The scale of $\text{Im}\{\beta\}$ is given by the relation $\text{Im}\{\beta\}|_{\text{MAX}} \approx 0.2$.

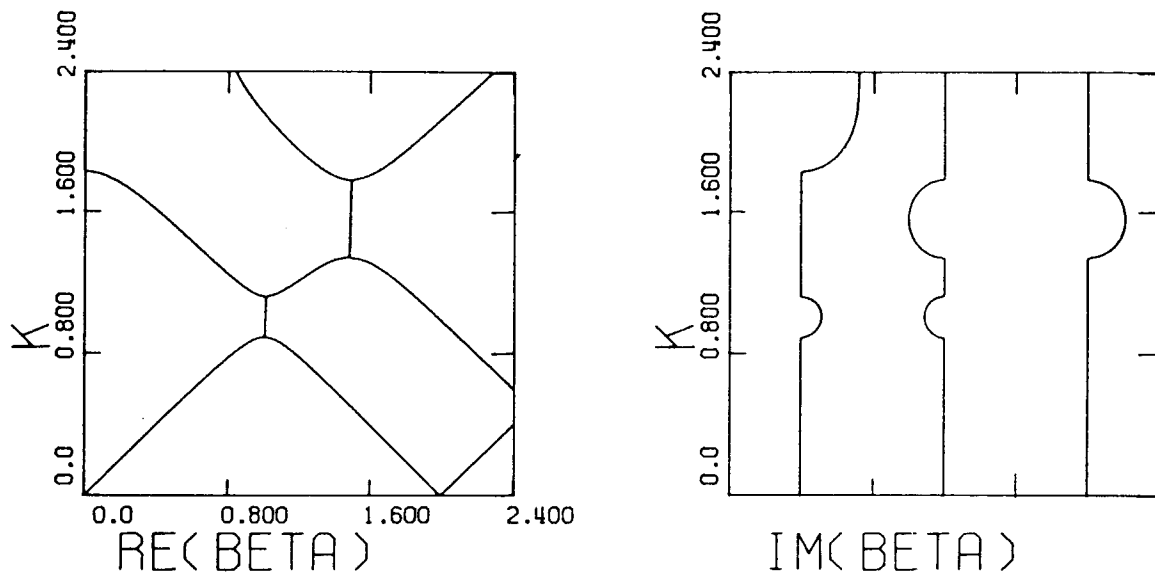


Figure 8. A plot of the Brillouin diagram for the almost periodic medium described by $\epsilon(z) = \epsilon_r \{1 + 0.5 \cos(\kappa_1 z) + 0.5 \cos[(\kappa_2 + \delta)z]\}$ where $\kappa_1 = 1.0$, $\kappa_2 = 1.5$, δ is irrational and $\delta \rightarrow 0$. The values of $\text{Re}\{\beta\}$ and $\text{Im}\{\beta\}$ are given in parts (a) and (b) respectively. The symbol K is defined by $K = k\epsilon_r^{1/2}$ on the graph. Various roots of the equation have various values for $\text{Im}\{\beta\}$. The scale of the three imaginary parts can be found from the relation $\text{Im}\{\beta\}|_{\text{MAX}} \approx 0.25$. The non-zero value of $\text{Im}\{\beta\}$ for $K > 1.9$ is an artifact due to the truncation of the first order theory.

where

$$\begin{aligned}\kappa_1 &= 2, & \kappa_2 &= 3 \\ \eta_1 &= 0.5, & \eta_2 &= 0.5\end{aligned}$$

It might be remarked that this dielectric constant is periodic and does not make sense for use in an almost periodic theory. This point, however, is moot as, to computer accuracy, there is no distinction between a rational and irrational number. The two theories, however, do make the distinction automatically as the rationality or irrationality of the ratio of the perturbation's spatial frequencies are inherent in the dispersion relation derivation. Clearly, the different forms of the two theories indicate that this is certainly the case. We, therefore, are allowed to make a direct comparison between two media whose difference the computer cannot distinguish.

A few words are necessary on how to read or interpret the diagrams 7 and 8. Figure 7 is similar to the usual Brillouin for single periodicities. That is, the real part of β , $\text{Re}\{\beta\}$, is represented by the solid line and the imaginary part of β , $\text{Im}\{\beta\}$, is represented by the dashed line. Regions where $\text{Im}\{\beta\}$ exists are called bandgaps and indicate that significant coupling between space harmonics does occur. The size of $\text{Im}\{\beta\}$ is directly proportional to the coupling per unit length for a given value of free space wavenumber k . As expected, there is large coupling in the vicinity of the Bragg wavenumbers $k \epsilon_r^{1/2} = \kappa_1/2 = 1$ and $k \epsilon_r^{1/2} = \kappa_2/2 = 3/2$. Figure 8 though is of a slightly different form. All roots of the dispersion relation are plotted since the numerical sorting of the multiple roots is difficult. The central root of $\text{Re}\{\beta\}$ is the desired root for comparison with the plot in Figure 7. The values for $\text{Im}\{\beta\}$ are plotted separately for each root. The constant portion of these plots represents the value $\text{Im}\{\beta\} = 0$. Again, two bandgaps appear, one each at the Bragg wavenumbers given before for the

periodic case. A third bandgap starting at $k \varepsilon_r^{1/2} \approx 1.9$ is an artifact due to the truncation of the first order almost periodic theory. It disappears when second order contributions are taken into account.

One interesting point noticeable on both plots is the greater size of the upper, with respect to the lower, bandgap. The ratio between the two sizes is seen to be very close to three halves. There is a simple reason for this. The coupling which is proportional to $\text{Im}\{\beta\}$ is always expressed per unit length. Because the wave sees more "bumps" per unit length at the higher frequency, it couples more strongly to the higher frequency perturbation linearly in a simple ratio of the frequencies. This result can be seen to be generally true, at least in the sense that the perturbations are small, from extended coupled-mode arguments presented elsewhere [18, 19, 21, 24].

The periodic and almost periodic theories appear to be essentially identical for the choice of parameters(24) used in Figures 7 and 8. However, consider the effect of phasing the two perturbations such that

$$f_N \rightarrow f_N \exp(i\phi_N) \quad (25)$$

The resulting periodic matrix \underline{D}_p has already been found to depend upon the phases ϕ_N [18, 19, 24]. However, the resulting almost periodic matrix is independent of phase as is evident from (23). Thus, in some sense, the two perturbations act independently in the almost periodic case as opposed to the periodic case.

The differences between the periodic and almost periodic theories will be placed in evidence when the bandgaps due to the two tones overlap. That is, for sufficiently small separation of tones or for sufficiently

large perturbation, the bandgaps will not act independently but instead will interfere. From coupled mode considerations we expect this overlap to occur whenever $\eta_1 + \eta_2 \gtrsim 8|\kappa_2 - \kappa_1|/(\kappa_2 + \kappa_1)$. To demonstrate this assertion, the Brillouin diagrams for the dielectric constant (24) with the parameters $\eta_1 = \eta_2 = 0.5$ and $\kappa_1 = 19$, $\kappa_2 = 20$ are given in Figures 9 and 10 for the two theories. For the almost periodic medium composed of two closely spaced tones and small perturbations, the dispersion relation (23) can be expanded in the vicinity of the Bragg wavenumbers to avoid numerical problems. The explicit relation plotted in Figure 10

$$\begin{aligned}
 (\tilde{\Delta\beta})^3 + \tilde{\Delta k}(\tilde{\Delta\beta})^2 - \tilde{\Delta\beta}[\tilde{\Delta k}^2 + \delta^2 - \eta_+^2/64] \\
 - \tilde{\Delta k}[\tilde{\Delta k}^2 - \delta^2 - \eta_+^2/64 - \delta\eta_-^2/64] = 0
 \end{aligned} \tag{26}$$

where

$$\tilde{\Delta\beta} = \beta/\kappa - 1/2$$

$$\tilde{\Delta k} = k\varepsilon_r^{1/2}/\kappa - 1/2$$

$$\eta_+^2 = |\eta_1|^2 + |\eta_2|^2$$

$$\eta_-^2 = |\eta_2|^2 - |\eta_1|^2$$

$$\delta = (\kappa_2 - \kappa_1)/(\kappa_1 + \kappa_2) = \Delta\kappa/2\kappa$$

is valid under the conditions

$$\eta_1, \eta_2 \ll 1$$

$$\Delta\kappa/\kappa \ll 1$$

$$\tilde{\Delta k} \ll 1$$

$$\tilde{\Delta\beta} \ll 1$$

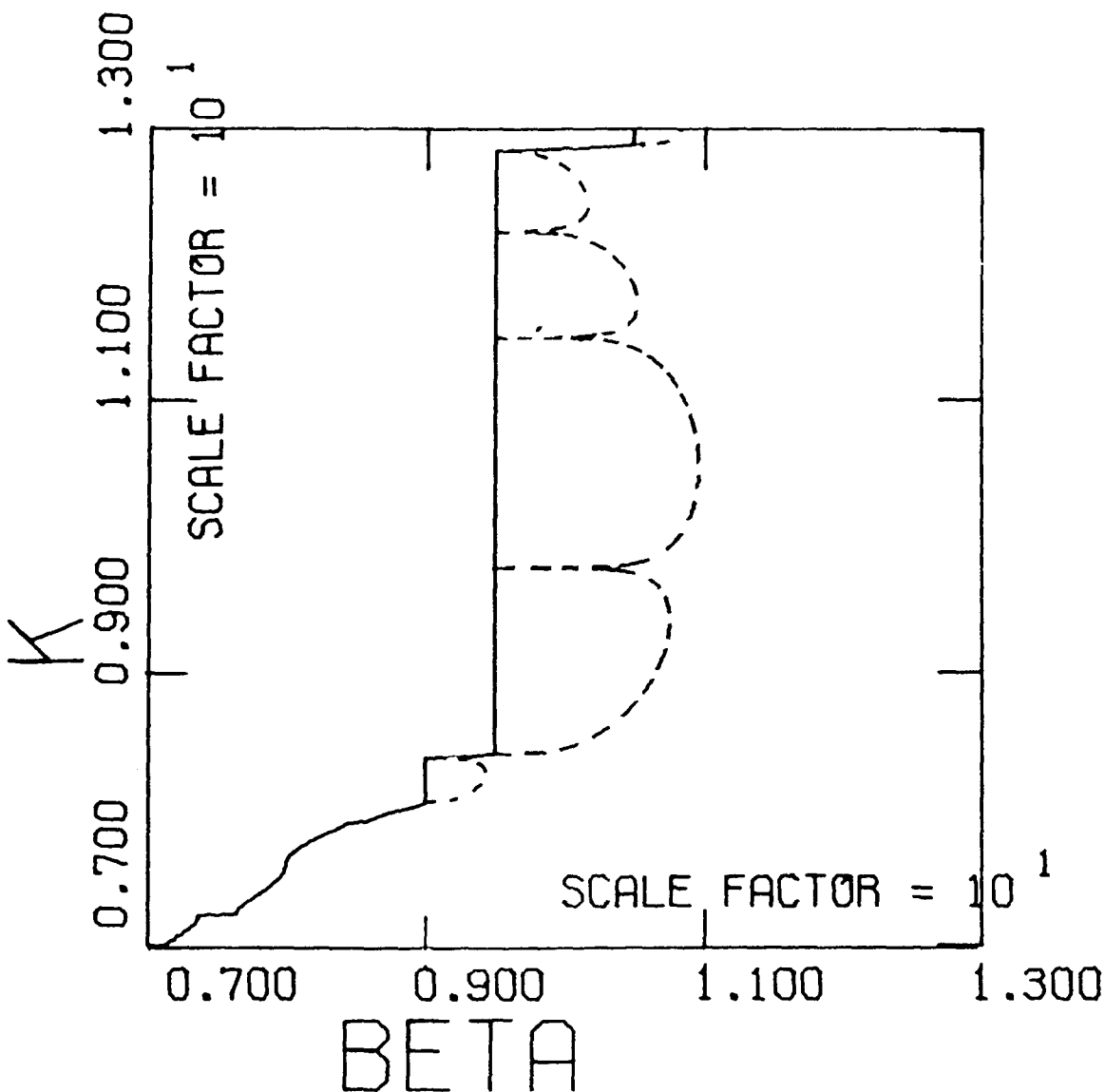


Figure 9. A plot of the Brillouin diagram for a periodic medium described by $\epsilon(z) = \epsilon_r [1 + 0.5 \cos(\kappa_1 z) + 0.5 \cos(\kappa_2 z)]$ where $\kappa_1 = 19.0$ and $\kappa_2 = 20.0$. The solid line represents values of $\text{Re}\{\beta\}$. The symbol K is defined by $K = k\epsilon_r^{1/2}$ on this graph. The scale of $\text{Im}\{\beta\}$ is given by the relation $\text{Im}\{\beta\}|_{\text{MAX}} = 1.4$.

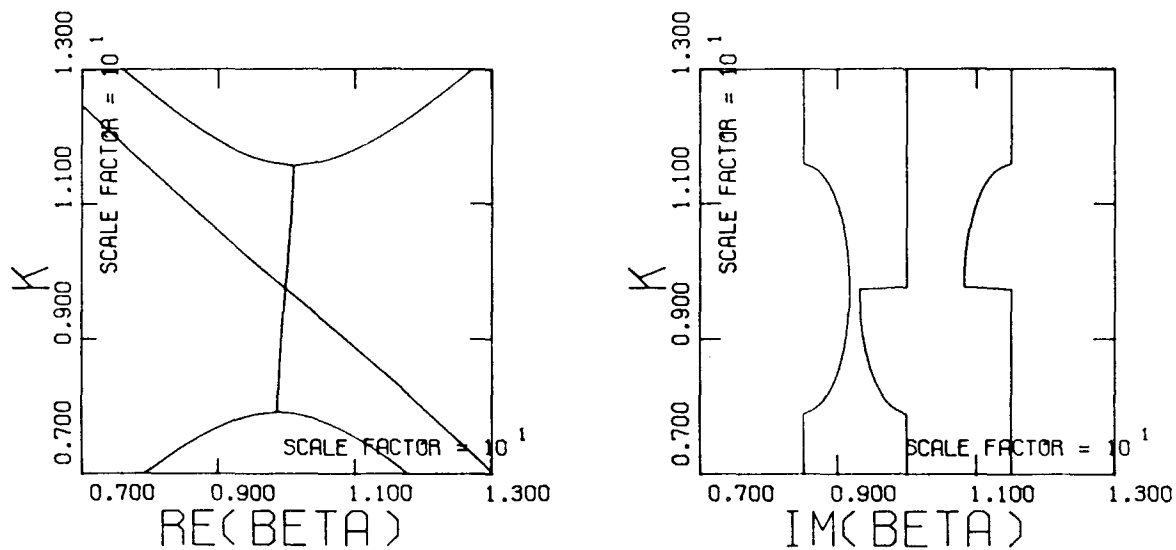


Figure 10. A plot of the Brillouin diagram for the almost periodic medium described by $\epsilon(z) = \epsilon_r \{1 + 0.5 \cos(\kappa_1 z) + 0.5 \cos[(\kappa_2 + \delta)z]\}$ where $\kappa_1 = 19.0$, $\kappa_2 = 20.0$, δ is irrational and $\delta \neq 0$. The values of $\text{Re}\{\beta\}$ and $\text{Im}\{\beta\}$ are given in parts (a) and (b) respectively. The symbol K is defined by $K = k\epsilon_r^{1/2}$ on this graph. Various roots of the equation have various values for $\text{Im}\{\beta\}$. The scale of the three imaginary parts can be found from the relation $\text{Im}\{\beta\}|_{\text{MAX}} = 1.7$.

A comparison of the plots in Figures 9 and 10 immediately demonstrates the difference in the two theories for closely spaced tones. In the periodic case, many bandgaps are formed as energy spills from the major interaction region to the many adjacent space harmonics. In this way, sub- and super-space harmonics are excited and participate in coupling whenever the perturbations are sufficiently large or the spacing of the tones is sufficiently small. In the (first order) almost periodic case only three space harmonics are present near the major interaction region. Therefore, there are exactly two bandgaps. For sufficiently large perturbations or for sufficiently small tone spacing (i.e., for $\eta_+ > 8\delta$) these two bandgaps merge into a single bandgap.

We expect that physically measurable quantities will reflect the properties and differences noted in the Brillouin diagrams for periodic and almost periodic media. For example, we expect that the reflection coefficient for periodic and almost periodic media will be similar unless the bandgaps overlap. For overlapping bandgaps, the reflection coefficients corresponding to the two theories will take on different characteristics. In particular, we expect that the reflection coefficient for the periodic case will have many large peaks, each one corresponding to a bandgap. However, in the almost periodic case, we expect the reflection coefficient to have only two main peaks which merge into a single peak under the constraint $\eta_+ \gtrsim 8\delta$. We expect the reflection from almost periodic media to be larger than the reflection from periodic media due to the larger imaginary wave-number in the almost periodic case. These applications of the theory will be treated in detail in another report.

IV. DISCUSSION AND CONCLUSIONS

A theory of electromagnetic wave propagation in almost periodic media is herein developed. The result takes the form of a dispersion relation that is explicitly illustrated for the first order (weakly perturbed) case when two tones are present. The Brillouin diagram is employed to compare and contrast this almost periodic theory with that of the well-known periodic theory.

Differences are noted between the results of the almost periodic and the periodic theory. The space harmonic coupling scheme is more complicated in the case of periodic media than almost periodic media. In fact, the almost periodic coupling scheme is found to be invariant with respect to arbitrary phasing of the perturbations in contradistinction to the periodic result. Although the calculated Brillouin diagrams of the two theories appear to be similar in a limit where the dimensionless tonal spacing is large compared to the perturbation, such is not the case in the band coalescence regime where the tonal spacing is small. In particular, only two stopbands appear in the almost periodic theory. These two stopbands coalesce in a smooth manner with decreasing tonal spacing. Such is not the case in the periodic theory where many stopbands may appear over a broad frequency range as the two tones approach a central limit. From these results, we surmise that the reflection coefficient for a periodic medium in the band coalescence regime should be broadband and possess a complicated structure whereas for almost periodic media the reflection coefficient would consist on one or at most two main peaks.

ACKNOWLEDGMENT

We acknowledge the helpful discussions with Professor C. H. Papas (Caltech). This research was supported by the National Science Foundation under Grant No. 76-14377.

REFERENCES

1. H. Bohr, C. R. 177, 737 (1923).
2. H. Bohr, C. R. 177, 1090 (1923).
3. H. Bohr, Acta Math. 45, 29 (1924).
4. H. Bohr, Acta Math. 46, 101 (1925).
5. H. Bohr, Acta Math. 47, 239 (1926).
6. A. Besicovitch, Acta Math. 47, 283 (1926).
7. S. Bochner, Proc. Lond. Math. Soc. 26, 433 (1926-27).
8. J. Favard, C. R. 182, 757 (1926).
9. J. Favard, C. R. 182, 1122 (1926).
10. J. Favard, J., Acta Math. 51, 131 (1927).
11. See, e.g., N. Minorsky, Nonlinear Oscillations, R. E. Kreiger Publishing Co., Huntington, N. Y. (1962).
12. H. Bohr, Almost Periodic Functions, trans. by H. Cohn and F. Steinhardt, Chelsea Publishing Co., New York (1947).
13. A. Besicovitch, Almost Periodic Functions, Cambridge University Press, London (1932).
14. N. Wiener, Generalized Harmonic Analysis-Tauberian Theorems, M.I.T. Press, Cambridge (1964).
15. A. Fink, Almost Periodic Differential Equations, Springer-Verlag, Berlin (1974).
16. J. Abel, Quart. J. Appl. Math. 28, 205 (1970).
17. J. Abel, J. Math. Anal. and Appl. 36, 110 (1971).
18. D. Jaggard and C. Elachi, J. Appl. Phys. 48, 1461 (1977).
19. D. Jaggard, Appl. Phys. 13, 185 (1977).
20. A. Mickelson, Ph.D. thesis, California Institute of Technology, Pasadena, California (1978).

21. See, e.g., D. Jaggard and G. Evans, Ant. Lab Rpt. No. 73 (1975), or D. Jaggard, Ant. Lab. Rpt. No. 75 (1976), California Institute of Technology, Pasadena, California.
22. G. Hill, Acta Math. VIII, 1 (1886), see also E. Whittaker and G. Watson A Course for Modern Analysis, 4th ed., Cambridge University Press, London (1927).
23. See, e.g., C. Kittel, Introduction to Solid State Physics, 5th ed., John Wiley and Sons, New York (1976).
24. D. Jaggard and C. Elachi, J. Opt. Soc. Am. 66, 674 (1976).